Functionalized Phosphanyl Complexes

DOI: 10.1002/anie.201002885

Insights into the Chemistry of Transient *P*-Chlorophosphanyl Complexes**

Aysel Özbolat-Schön, Maren Bode, Gregor Schnakenburg, Anakuthil Anoop, Maurice van Gastel, Frank Neese,* and Rainer Streubel**

Dedicated to Professor Michael F. Lappert

Main-group-element compounds with one or more unpaired electrons have emerged as a fascinating research topic in recent years.[1,2] The fundamental breakthrough in the area of phosphorus-based radicals with low-coordinate phosphorus centers[3] was achieved by M. F. Lappert et al. with the synthesis of the first stable derivative of type **I** (R = $CH(SiMe_3)_2$),[4] which dimerizes (reversibly) upon crystallization.[5] This compound has been used as a ligand in cobalt and iron carbonyl complexes.[6] More recently, heteroatom-substituted derivatives of **II**[7] and **III**[8] have been synthesized (Scheme 1). Interesting follow-up reactions involving rearrangement and decomposition processes of **III** have been observed. In contrast, knowledge about derivatives **IV**,[9,10] which have potential leaving groups, is extremely scarce and, to the best of our knowledge, its coordination chemistry is unknown. The latter is of special interest, as open-shell complexes have been recognized as highly interesting targets, for example as contrast agents for molecular imaging.[11]

Our current investigations of Li/Cl-phosphinidenoid complex chemistry[12–16] has led us to the discovery of transient *P*-chlorophosphanyl complexes formed by one-electron oxidation. These transient complexes undergo combined cross-coupling/rearrangement and cross-coupling/elimination reactions, which in the latter case yielded the first structurally characterized derivative of a phosphaquinomethane complex.

P-Chlorophosphane complexes **1a**[17] and **1b**[18] were transformed into the *P*-chlorophosphinidenoid complexes **2a**,**b** using LDA/[12]crown-4,[12,14] and then treated with tritylium tetrafluoroborate at low temperature. Slow warm-up yielded the complexes **5** and **6**, which were isolated using column chromatography. The proposed reaction pathway is shown in Scheme 2 and involves the formation of a radical pair consisting of the tritylium radical and the *P*-chlorophosphanyl complexes **3a**,**b** upon oxidation. After a C,P coupling reaction leading to complexes **4a**,**b**, either a subsequent H-translocation occurs to form complex **5** or HCl elimination takes place to give complex **6**. The presence of the open-shell intermediates **3a**,**b** was confirmed by ESR spectroscopic and DFT investigations (see below).

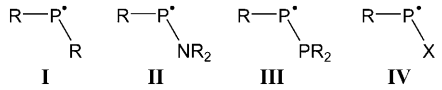

Scheme 1. Low-coordinate phosphorus radicals without (**I**) and with *P*-functional groups such as $-NR_2$ (**II**), $-PR_2$ (**III**), and -X (**IV**). X denotes OR or halogen.

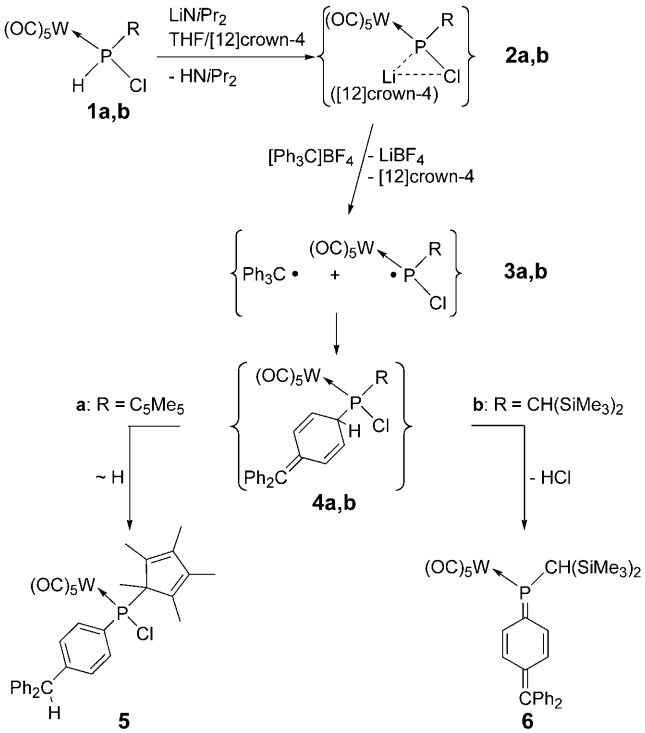

Scheme 2. Proposed pathway for the reaction of phosphinidenoid complexes **2a**,**b** with tritylium tetrafluoroborate to yield transient *P*-chlorophosphanyl complexes **3a**,**b** and subsequently complexes **5** and **6**.

[*] A. Özbolat-Schön, Dr. M. Bode, Dr. G. Schnakenburg, Prof. Dr. R. Streubel
Institut für Anorganische Chemie der Rheinischen Friedrich-Wilhelms-Universität Bonn
Gerhard-Domagk-Strasse 1, 53121 Bonn (Germany)
Fax: (+49) 228-739-616
E-mail: r.streubel@uni-bonn.de
Dr. A. Anoop, Dr. M. van Gastel, Prof. Dr. F. Neese
Institut für Physikalische und Theoretische Chemie der Rheinischen Friedrich-Wilhelms-Universität Bonn
Wegeler Strasse 12, 53115 Bonn (Germany)

[**] Financial support by the Deutsche Forschungsgemeinschaft (SFB 813 "Chemistry at Spin Centers", TP A4 and B4), the Fonds der Chemischen Industrie, and the COST action cm0802 "PhoSciNet" is gratefully acknowledged.

Supporting information for this article is available on the WWW under http://dx.doi.org/10.1002/anie.201002885.

We also examined whether the reaction pathway is dependent on the stoichiometry. Using complex **1b**, we observed that upon increasing the amount of the tritylium salt from 1.24 to 3.20 equivalents, two new complexes **8** and **9** (in ratio 1:4) were formed. Whereas **8** was easily identified by ^{31}P NMR spectroscopy because of its chemical shift ($\delta =$ 213.0 ppm) and the phosphorus–tungsten and phosphorus–fluorine coupling constants ($^{1}J_{W,P} = 347.0$ Hz, $^{1}J_{P,F} =$ 1015.8 Hz), the structure of complex **9** (128.3 ppm, $^{1}J_{W,P} =$ 270.8 Hz) could not be identified.[19] We assume that oxidation of complex **3b** took place leading to the formation of transient *P*-chlorophosphenium complex **7** and finally to complex **8** (Scheme 3).

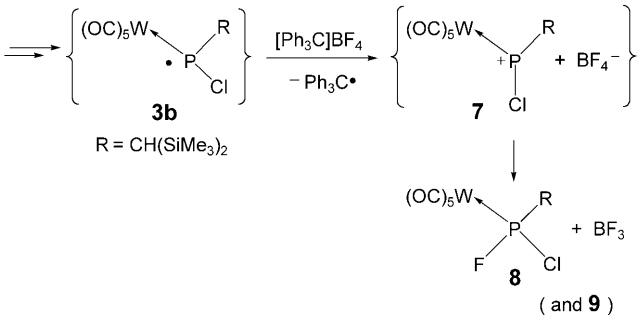

Scheme 3. Proposed reaction of transient *P*-chlorophosphanyl complex **3b** with tritylium tetrafluoroborate to yield transient complex **7** and subsequently complexes **8** and **9**.

The ^{1}H NMR spectrum of complex **5** revealed a signal at $\delta = 5.66$ ppm, next to the two signals in the aromatic region, which was assigned to the proton at the aliphatic carbon center of the former trityl group. In contrast, two signals at 6.80 ppm ($^{3}J_{P,H} = 6.60$ Hz, $^{3}J_{H,H} = 9.78$ Hz, $^{4}J_{H,H} = 1.71$ Hz) and 7.02 ppm ($^{3}J_{P,H} = 9.88$ Hz, $^{3}J_{H,H} = 9.74$ Hz, $^{4}J_{H,H} = 1.84$ Hz) were observed for complex **6**, which were assigned to the quinone-type protons in the β position to phosphorus. Interestingly, complex **6** showed an intense purple color ($\lambda_{max} =$ 525 nm), which is in strong contrast to the color of non-coordinated phosphaquinomethane derivatives,[20] which have yellow to orange colors with λ_{max} values between 372 and 440 nm.

The molecular structures of complexes **5** and **6** were unambiguously established by single-crystal X-ray diffraction studies (Figure 1 and Figure 2).

Whereas the C–C bond lengths in complex **5** for the ring system bound to the pyramidal phosphorus center indicate a typical aromatic system (1.389(5)–1.411(6) Å), the alternating bond lengths in complex **6** confirm a quinone-type character and a planar coordination geometry at phosphorus (bond angle sum at phosphorus: 358.8°).[21] The P–C8 bond length (1.716(4) Å) is in the range of a long P–C double bond (1.61–1.71 Å)[22] and is typical for phosphaquinomethane compounds.[20b,c] Whereas C13–C12 (1.358(5) Å) and C9–C10 (1.350(5) Å) have rather typical C–C double-bond values, the lengths of C8–C9, C8–C13, C12–11, and C10–C11 are in accordance with those expected for C–C single bonds.

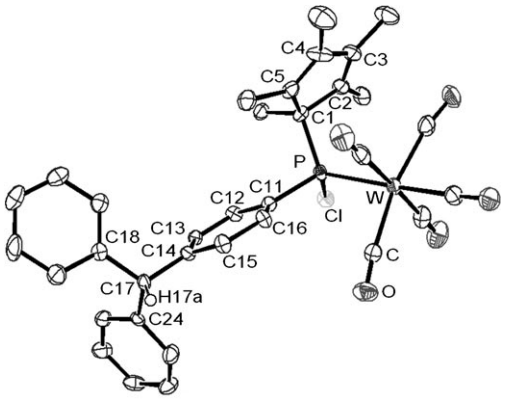

Figure 1. Structure of complex **5** (ellipsoids set at 50% probability; hydrogen atoms except H17a omitted for clarity). Selected bond lengths [Å] and angles [°]: W–P 2.520(1), P–Cl 2.073(1), P–C1 1.864(4), P–C11 1.829(4), C11–C12 1.411(6), C11–C16 1.395(5), C12–C13 1.389(5), C13–C14 1.391(5), C14–C15 1.394(6), C14–C17 1.521(5), C15–C16 1.396(5); C1-P-C(11) 105.32(19), C1-P-Cl 102.23(14), C11-P-Cl 99.10(13), C1-P-W 119.88(14), C11-P-W 115.47(13), Cl-P-W 112.13(5).

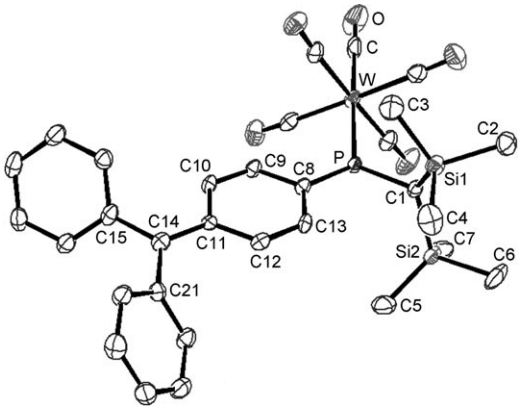

Figure 2. Structure of complex **6** (ellipsoids set at 50% probability; hydrogen atoms omitted for clarity). Selected bond lengths [Å] and angles [°]: W–P 2.4929(9), P–C1 1.828(4), P–C8 1.716(4), C8–C9 1.430(5), C8–C13 1.440(5), C9–C10 1.350(5), C10–C11 1.460(5), C11–C12 1.434(5), C12–C13 1.358(5), C11–C14 1.407(5), C14–C15 1.482(5), C14–C21 1.475(5); C1-P-W 121.32(13), C1-P-C8 112.00(18), W-P-C8 125.49(13).

Interestingly, the length of the C11–C14 bond (1.407(5) Å) indicates an elongated double bond.

Using ESR spectroscopy, we were able to obtain further information about the transient radical species. We observed hyperfine phosphorus couplings that were attributed to complex **3a** ($a_{iso} = 280$ MHz, $a_{dip,\perp} = -280$ MHz, $a_{dip,\parallel} =$ 560 MHz, $g = 2.001(2)$) and **3b** ($a_{iso} = 137$ MHz, $a_{dip,\perp} =$ -314 MHz, $a_{dip,\parallel} = 629$ MHz, $g = 2.002(2)$). An ESR spectrum of **3b** in liquid solution is shown in Figure 3. The average *g* values of the liquid-solution spectra are typical for organic radicals. Their exact value is determined by the amount of spin population at phosphorus and its ligand field, in analogy to ligand-field splitting in the case of transition metals. They agree well with typical *g* values of ^{31}P radicals, which range

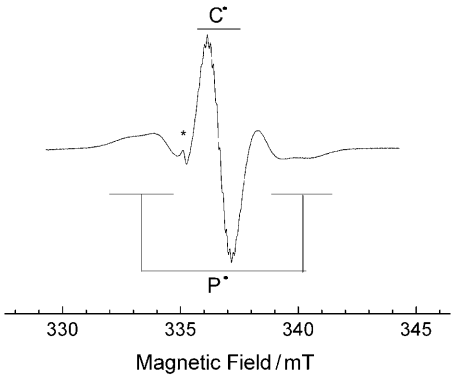

Figure 3. ESR spectrum of **3b** in THF at 150 K. Parameters: $\nu_{mw} = 9.456$ GHz, $P_{mw} = 2$ mW, modulation amplitude = 1 mT. The carbon-centered radical corresponds to a trityl radical (see Scheme 2 and Supporting Information). The signal marked with an asterisk corresponds to a paramagnetic impurity present in the solution.

from 1.999 up to 2.01 depending on the coordination number of ^{31}P.[9]

At 165 K, a correlation (R factor = 87%) is observed in the time evolution of the ESR spectra (Figure 4a), in which the decrease of signal of the P-centered radical correlates with the increase of the signal of the trityl radical. This indicates that P-centered radicals are present initially, but then convert into the trityl radical during the course of the reaction; the spectrum of the trityl radical is shown in Figure 4b.

Analysis of the hyperfine coupling constants is best performed in combination with density functional theory (DFT).[23] Spin-density distributions[24] resulting from DFT calculations for **3a** and **3b** are shown in Figure 5 (the data for the $Ph_3C^•$ radical are given in the Supporting Information). The experimentally observed ^{31}P hyperfine coupling constants indicate an electron spin population of 86% for **3b** and essentially planar local environments of the phosphorus

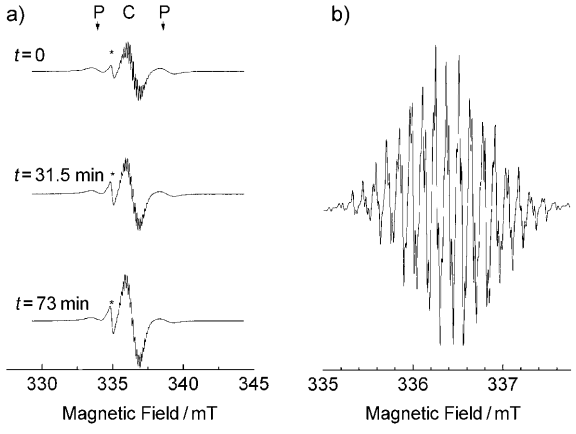

Figure 4. a) ESR spectra of the reaction solution of **3b** recorded after addition of excess of tritylium tetrafluoroborate and at time intervals $t = 31.5$ min and $t = 73$ min. The intensity of the signal due to the trityl radical increases with time whereas those of the phosphorus-centered radicals decrease. Parameters: $T = 165$ K, $\nu_{mw} = 9.456$ GHz, $P_{mw} = 2$ mW, modulation amplitude = 1 mT. b) ESR signal of the trityl radical recorded at 165 K and with a modulation amplitude of 0.1 mT.

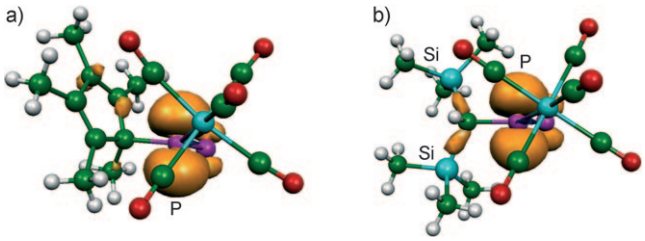

Figure 5. Calculated spin-density distribution for complexes **3a** and **3b.** The Mulliken spin populations from DFT calculations at ^{31}P amount to 87% and 82%, respectively. C green, H white, W,Si cyan, O red, P,Cl magenta; spin density is given in orange.

center with a sp^2 hybridization and the unpaired electron in a pure 3p orbital. This observation is in good agreement with the DFT calculations, where 82% spin population is found. For **3a**, DFT calculations indicate that the unpaired electron is partially delocalized over the C_5Me_5 moiety, with the exact amount of delocalization depending on whether the phosphorus coordinates to one or two carbon atoms of the C_5Me_5 ring. From analysis using the model described in the experimental section, the electron spin population amounts to 76% for **3a** and DFT calculations give rise to 87% spin population. The coordination geometry of P in **3a** is slightly more bent than in **3b**.

In conclusion, the formation of transient P-substituted phosphanyl complexes with a trigonal-planar coordination environment and with an unpaired electron in a 3p(P) orbital was demonstrated by a combination of synthetic and spectroscopic approaches. DFT calculations reveal that the spin distribution of the radical complexes is strictly depending on the nature of the substituent at phosphorus. Currently, we are working on a fine-tuning of the system Li/Cl phosphinidenoid complex/single-electron-transfer oxidant for various applications.

Experimental Section

All operations were performed in an atmosphere of purified and dried argon. Solvents were distilled from sodium. NMR data were recorded on a Bruker Avance 300 spectrometer at 25°C using $CDCl_3$ (**5**) or CD_2Cl_2 (**6**) as solvent and internal standard; chemical shifts δ are given relative to tetramethylsilane (^{13}C: 75.5 MHz) and 85% H_3PO_4 (^{31}P: 121.5 MHz). ESR spectroscopy: X-band (9 GHz) continuous wave (cw) ESR spectra were recorded either in liquid or in frozen solution on a Bruker ESP300E ESR spectrometer with a rectangular 4102ST cavity and an Oxford ESR910 flow cryostat. Isotropic and dipolar ^{31}P hyperfine coupling constants and average g values (in liquid solution) were extracted directly from the spectra. Infrared spectra were collected on FT-IR Nicolet 380. Mass spectra were recorded on a Kratos Concept 1H spectrometer. Elemental analyses were performed using an Elementa (Vario EL) analytical gas chromatograph.

5 and **6**: Lithium diisopropylamide (LDA, 1.1 mmol), freshly synthesized using *n*-butyllithium 1.6 mol L^{-1} solution in *n*-hexane; 0.7 mL, 1.1 mmol) and diisopropylamine (160 μL, 1.1 mmol) in diethyl ether (1 mL) were dissolved in THF (8 mL) and cooled to −90°C. A solution of of **1a** (527 mg, 1.0 mmol) or of **1b** (551 mg, 1.0 mmol) and (162 μL, 1.0 mmol) [12]crown-4 in THF (8 mL) was then added to the LDA solution. After adding tritylium tetrafluor-

oborate ($[Ph_3C]BF_4$; 410 mg, 1.24 mmol) to the solution of **2a** or **2b** at −80 °C, an immediate color change from orange to red to dark Bordeaux red/violet was observed. The reaction mixtures were allowed to stir while gently warming to ambient temperature to yield a light red (for **5**) or dark purple solution (for **6**). After evaporation and low-temperature column chromatography (**5**: −20 °C; Al_2O_3 using the following eluents: 1) petroleum ether, 2) petroleum ether/diethyl ether 95:5, and 3) 90:10; **6**: −20 °C; SiO_2 using pure petroleum ether), complexes **5** and **6** were obtained as solids after removal of solvent in vacuo.

5: Pale yellow solid; yield: 440 mg (0.57 mmol, 57 %); m.p. 158 °C (decomp.); selected NMR data: $^{13}C\{^1H\}$ NMR: $\delta = 10.7$ (d, $J_{P,C} = 1.9$ Cp*-CH_3), 10.8 (d, $J_{P,C} = 1.6$ Hz, Cp*-CH_3), 11.3 (d, $J_{P,C} = 0.8$ Hz, Cp*-CH_3), 12.2 (d, $J_{P,C} = 1.6$ Hz, Cp*-CH_3), 12.9 (d, $^3J_{P,C} = 5.0$ Hz, Cp*(C1)-CH_3), 55.5 (d, $^5J_{P,C} = 1.4$ Hz, $CHArPh_2$), 63.6 (d, $^1J_{P,C} = 2.3$ Hz, Cp*(C1)), 125.6 (s, *p*-Ph), 127.4 (d, $J_{P,C} = 14.7$ Hz, Ar), 127.5 (s, *o*-Ph), 128.4 (s, *m*-Ph), 132.4 (d, $J_{P,C} = 15.8$ Hz, Ar), 132.7 (d, $^1J_{P,C} = 18.5$ Hz, *i*-Ar), 133.0 (d, $J_{P,C} = 6.5$ Hz, Cp*), 138.7 (d, $J_{P,C} = 4.3$ Hz, Cp*), 141.2 (d, $J_{P,C} = 6.8$ Hz, Cp*), 142.0 (d, $J_{P,C} = 3.6$ Hz, *i*-Ph), 143.7 (d, $J_{P,C} = 8.7$ Hz, Cp*), 146.9 (d, $^4J_{P,C} = 2.6$ Hz, *p*-Ar-$CHPh_2$), 195.2 (d_{sat}, $^2J_{P,C} = 7.1$ Hz, $^1J_{W,C} = 126.7$ Hz, *cis*-CO), 196.8 ppm (d, $^2J_{P,C} = 32.9$ Hz, *trans*-CO); $^{31}P\{^1H\}$ NMR: $\delta = 114.5$ ppm (s_{sat}, $^1J_{W,P} = 279.7$ Hz); MS: *m*/*z* (%): 768 (1) [M^+]; IR (KBr; ν(CO)): $\tilde{\nu} = 1931$ (s), 1988 (m), 2073 (m) cm^{-1}. Elemental analysis (%) calcd for $C_{34}H_{30}ClPO_5W$: C 53.11, H 3.93; found: C 52.95, H 3.81.

6: purple, air-sensitive solid; yield: 475 mg (0.63 mmol, 63 %); m.p. 169 °C (decomp.); selected NMR data: $^{13}C\{^1H\}$ NMR: $\delta = 2.3$ (d, $^3J_{P,C} = 2.6$ Hz, $SiMe_3$), 34.7 (dd, $^1J_{P,C} = 13.9$ Hz, P*C*H), 124.3 (d, $^2J_{P,C} = 34.9$, *C*H), 126.2 (d, $^3J_{P,C} = 42.1$ Hz, *C*H), 127.5 (m, Ph/CH), 128.0 (m, Ph/CH), 130.0 (s, Ph), 131.4 (s, Ph), 131.5 (s, Ph), 134.2 (d, $^4J_{P,C} = 32.5$ Hz, *C*=C-Ph_2), 141.7 (s, *i*-Ph), 142.6 (d, $^5J_{P,C} = 8.9$ Hz, C=*C*Ph_2), 142.7 (s, *i*-Ph), 163.9 (d, $^1J_{P,C} = 48.5$ Hz, P=*C*), 196.2 (d_{sat}, $^1J_{W,C} = 125.5$ Hz, $^2J_{P,C} = 13.2$ Hz, *cis*-CO), 200.3 ppm (d, $^2J_{P,C} = 30.0$ Hz, *trans*-CO); $^{31}P\{^1H\}$ NMR: $\delta = 189.6$ ppm (s_{sat}, $^1J_{W,P} = 269.5$ Hz); MS: *m*/*z* (%): 756 (28) [M^+]; IR (nujol; ν(CO)): $\tilde{\nu} = 1941$ (s), 1981 (m), 2068 (m) cm^{-1}; elemental analysis (%) calcd for $C_{31}H_{33}PO_5Si_2W$: C 49.21, H 4.40; found: C 48.95, H 4.21.

For X-ray analysis data of complexes **5** and **6** and the synthesis of complexes **8** and **9**, see the Supporting Information.

Analysis of experimental hyperfine coupling constants: The anisotropic hyperfine coupling constants give direct information about the amount of $^{31}P(3p)$ character of the singly occupied molecular orbital. The constants $a_{dip,\perp}$ and $a_{dip,\parallel}$ are related to the 3p spin density at ^{31}P according to reference [25] [Eq. (1) and (2)]:

$$a_{dip,\parallel} = 4/5(917\,MHz)\,\rho(^{31}P(3p)) \quad (1)$$

$$a_{dip,\perp} = -2/5(917\,MHz)\,\rho(^{31}P(3p)) \quad (2)$$

The isotropic hyperfine interaction $a_{iso}(^{31}P)$, visible in the ESR spectra of the liquid solution, derives from two origins. First, owing to spin polarization mechanisms, the $^{31}P(3p)$ spin population also causes the presence of a small amount of $^{31}P(3s)$ spin population. The amount of $^{31}P(3s)$ spin population by polarization is estimated by a McConnell-like relation using a value of 1.13 % spin polarization [Eq. (3)]:[25]

$$\rho_{pol}(^{31}P(3p)) \approx 0.0113\,\rho(^{31}P(3p)) \quad (3)$$

Further 3s spin density may be introduced if the local environment of phosphorus is not planar. In this case, the sp^2 hybridization scheme is no longer valid and a direct contribution of the 3s orbital in the wavefunction of the unpaired electron is expected. The total spin population in the 3s orbital gives rise to an isotropic hyperfine coupling constant [Eq. (4)]:

$$a_{iso}(^{31}P) = (13\,306\,MHz)\,\rho_{tot}(^{31}P(3s)) \quad (4)$$

Received: May 12, 2010
Published online: August 16, 2010

Keywords: EPR spectroscopy · phosphanyl complexes · phosphaquinomethane · phosphinidenoid complexes · tritylium salts

[1] Reviews: a) V. Ya Lee, M. Nakamoto, A. Sekiguchi, *Chem. Lett.* **2008**, *37*, 128; b) J. Iley in *The Chemistry of Organic Germanium, Tin and Lead Compounds* (Eds.: S. Patai, Z. Rappoport), Wiley, Chichester, **1995**, chap. 5; c) P. P. Power, *Chem. Rev.* **2003**, *103*, 789 – 809; d) H. Grützmacher, F. Breher, *Angew. Chem.* **2002**, *114*, 4178 – 4184; *Angew. Chem. Int. Ed.* **2002**, *41*, 4006 – 4011.

[2] Recent examples of Group 14 element radicals: a) C. Drost, J. Griebel, R. Kirmse, P. Lönnecke, J. Rheinhold, *Angew. Chem.* **2009**, *121*, 1996 – 1999; *Angew. Chem. Int. Ed.* **2009**, *48*, 1962 – 1965; b) C. Förster, K. W. Klinkhammer, B. Tumanskii, H.-J. Krüger, H. Kelm, *Angew. Chem.* **2007**, *119*, 1174 – 1177; *Angew. Chem. Int. Ed.* **2007**, *46*, 1156 – 1159.

[3] S. Marque, P. Tordo, *Top. Curr. Chem.* **2005**, *250*, 43 – 76.

[4] M. J. S. Gynane, A. Hudson, M. F. Lappert, P. P. Power, H. Goldwhite, *J. Chem. Soc. Chem. Commun.* **1976**, 623 – 624.

[5] S. L. Hinchley, C. A. Morrison, D. W. H. Rankin, C. L. B. Macdonald, R. J. Wiacek, A. H. Cowley, M. F. Lappert, G. Gundersen, J. A. C. Clyburne, P. P. Power, *Chem. Commun.* **2000**, 2045 – 2046.

[6] A. H. Cowley, R. A. Kemp, J. C. Wilburn, *J. Am. Chem. Soc.* **1982**, *104*, 332 – 334.

[7] a) M. J. S. Gynane, A. Hudson, M. F. Lappert, P. P. Power, H. Goldwhite, *J. Chem. Soc. Dalton Trans.* **1980**, 2428 – 2433; b) J.-P. Bezombes, K. B. Borisenko, P. B. Hitchcock, M. F. Lappert, J. E. Nycz, D. W. H. Rankin, H. E. Robertson, *Dalton Trans.* **2004**, 1980 – 1988.

[8] S. Loss, A. Magistrato, L. Cataldo, S. Hoffmann, M. Geoffroy, U. Röthlisberger, H. Grützmacher. *Angew. Chem.* **2001**, *113, 749–751; Angew. Chem. Int. Ed.* **2001**, 40, 723 – 726; *Angew. Chem. Int. Ed.* **2001**, *40*, 723 – 726.

[9] B. Cetinkaya, A. Hudson, M. F. Lappert, H. Goldwhite, *J. Chem. Soc. Chem. Commun.* **1982**, 609 – 610.

[10] Reduction of dihalo(organo)phosphanes might yield *P*-functionalized phosphanyl radicals as transient species, but only subsequently formed products have been unambigously identified to date; see for example: J. Geier, H. Rüegger, M. Wörle, H. Grützmacher, *Angew. Chem.* **2003**, *115*, 4081 – 4085; *Angew. Chem. Int. Ed.* **2003**, *42*, 3951 – 3954, and references therein.

[11] K. E. Torraca, L. McElwee-White, *Coord. Chem. Rev.* **2000**, *206–207*, 469 – 491.

[12] A. Özbolat, G. von Frantzius, J. Marinas-Perez, M. Nieger, R. Streubel, *Angew. Chem.* **2007**, *119*, 9488 – 9491; *Angew. Chem. Int. Ed.* **2007**, *46*, 9327 – 9330.

[13] A. Özbolat, G. von Frantzius, W. Hoffbauer, R. Streubel, *Dalton Trans.* **2008**, 2674 – 2676.

[14] M. Bode, J. Daniels, R. Streubel, *Organometallics* **2009**, *28*, 4636 – 4638.

[15] R. Streubel, A. Özbolat-Schön, M. Bode, J. Daniels, G. Schnakenburg, F. Teixidor, C. Vinas, A. Vaca, A. Pepiol, P. Farras, *Organometallics* **2009**, *28*, 6031 – 6035.

[16] C. Albrecht, M. Bode, J. M. Pérez, G. Schnakenburg, R. Streubel, unpublished results.

[17] R. Streubel, S. Priemer, F. Ruthe, P. G. Jones, *Eur. J. Inorg. Chem.* **2000**, 1253 – 1259.

[18] R. Streubel, U. Rhode, J. Jeske, F. Ruthe, P. G. Jones, *Eur. J. Inorg. Chem.* **1998**, 2005 – 2012.

[19] The $^{31}P\{^{1}H\}$ NMR signal at $\delta = 128$ ppm has a shoulder (ratio ca. 3:1) that was attributed to ^{35}Cl and ^{37}Cl isotopomers, thus indicating a phosphorus–chlorine bond.
[20] a) G. Märkl, R. Hennig, K. M. Raab, *Chem. Commun.* **1996**, 2057 – 2058; b) F. Murakami, S. Sasaki, M. Yoshifuji, *J. Am. Chem. Soc.* **2005**, *127*, 8926 – 8927; c) S. Sasaki, F. Murakami, M. Yoshifuji, *Angew. Chem.* **1999**, *111*, 351 – 354; *Angew. Chem. Int. Ed.* **1999**, *38*, 340 – 343.
[21] This is in contrast to the related complex $[(OC)_5WP(R)CN\{Li[12]crown\text{-}4\}]$ ($R = CH(SiMe_3)_2$) featuring three-coordinate phosphorus with a pyramidal geometry (bond angle sum at phosphorus: 311.5°): A. Özbolat, G. von Frantzius, E. Ionescu, S. Schneider, M. Nieger, P. G. Jones, R. Streubel, *Organometallics* **2007**, *26*, 4021 – 4024.
[22] a) R. Appel, in *Multiple Bonds and Low Coordination in Phosphorus Chemistry* (Eds.: M. Regitz, O. J. Scherer), Thieme, Stuttgart, **1990**, pp. 157 – 219; b) M. Yoshifuji, *J. Chem. Soc. Dalton Trans.* **1998**, 3343 – 3350; c) P. P. Power, *Chem. Rev.* **1999**, *99*, 3463 – 3503.
[23] DFT calculations have been performed on models of **3a** and **3b** and $PhC_3^{\bullet}$ based on the crystal structures. All the calculations were performed using the ORCA Program package (F. Neese, University of Bonn, 2010) and employ the BP functional and a TZVP basis set within a spin-unrestricted Kohn–Sham formalism.
[24] The term spin-density distribution refers to the spin density as a function of three-dimensional space, as depicted in Figure 5. The term (Mulliken) spin population refers to its coefficients; for example, in case of **3a**, the unpaired electron resides up to 87% at a P(3p) orbital.
[25] J. R. Morton, K. F. Preston, *J. Magn. Reson.* **1978**, *30*, 577 – 582.
[26] J. H. van der Waals, G. ter Maten, *Mol. Phys.* **1964**, *8*, 301 – 318.

